Pathol. Oncol. Res. (2012) 18:793–802
DOI 10.1007/s12253-012-9505-0

RESEARCH

Characterization of a New Human Cell Line (CH-3573) Derived from a Grade II Chondrosarcoma with Matrix Production

Silvia Calabuig-Fariñas · Rosario Gil Benso · Karoly Szuhai · Isidro Machado · José Antonio López-Guerrero · Danielle de Jong · Amando Peydró · Teresa San Miguel · Lara Navarro · Antonio Pellín · Antonio LLombart-Bosch

Received: 5 November 2011 / Accepted: 17 January 2012 / Published online: 15 February 2012

Abstract Chondrosarcomas are malignant cartilage-forming tumors that represent the third most common malignant solid tumor of bone. In patients with grades II and III, local recurrence, increasing tumor size and dedifferentiation have been associated with lower survival rates. These biologically poorly-understood neoplasms vary considerably in clinical presentation and biological behavior. Cytogenetic studies have shown that heterogeneity is related to karyotypic complexity; moreover, alterations in the 9p21 locus and *TP53* gene are related to disease progression. Despite the relatively high frequency of chondrosarcoma only a limited number of cell lines exist in the scientific community, limiting the possibility to study hypothesis-derived research or primary drug interaction necessary for pre-clinical studies. We report a chondrosarcoma cell line, CH-3573, derived from a primary tumor that may serve as a useful tool for both in vitro and in vivo models to study the molecular pathogenesis. In addition, xenograft passages in nude mice were studied to characterize the genetic stability over the course of tumor progression. In contrary to other reported cell lines, an important feature of our established cell line was the retained matrix production, a characteristic feature of a conventional grade II chondrosarcoma. The cell line (CH-3573) was characterized by pathological, immunohistochemical and molecular genetic methods.

Keywords Bone tumor · Cell line · Chondrosarcoma · Grade II · Karyotype · Matrix

S. Calabuig-Fariñas · R. G. Benso · I. Machado · A. Peydró · T. S. Miguel · L. Navarro · A. Pellín · A. LLombart-Bosch (✉)
Department of Pathology, University of Valencia,
Avda. Blasco Ibañez, 17,
46010 Valencia, Spain
e-mail: antonio.llombart@uv.es

K. Szuhai · D. de Jong
Department of Molecular Cell Biology,
Leiden University Medical Centre,
Leiden, The Netherlands

J. A. López-Guerrero
Laboratory of Molecular Biology,
Fundación Instituto Valenciano de Oncología,
Valencia, Spain

Introduction

Chondrosarcomas (CHS) are malignant cartilage-forming tumors that represent the third most common malignant tumor of bone after myeloma and osteosarcoma; constituting approximately 11% of this group of tumors. CHS form a heterogeneous group of neoplasms and are classified according to the origin, anatomic location, size of the lesion and histological grade following the Evans grading scheme [1]. Conventional CHS are subdivided into grade I, II and III, based upon cellularity, mitotic rate and cellular atypia. The histological diagnosis and grading of CHS is frequently difficult, and the histological appearance does not always reflect the biological behavior of these tumors [2]. Nearly 90% of CHS are grade I or II, with relatively slow growth and low metastatic potential, and usually occur in patients older than 50 years [3]. Conventional treatment of malignant CHS based on surgery, current chemotherapy drugs and

radiation therapy are generally ineffective. Furthermore, there is no treatment available for patients with metastatic disease or inoperable tumors in the extremities, trunk or pelvis [4]. For these reasons it is very important to characterize new cell models in order to understand the biological characteristics and behavior of CHS. To our knowledge, seven CHS cell lines have been established between 1989 and 2009: one secondary CHS derived from Ollier's disease, three grade III CHS and three dedifferentiated CHS; most are characterized by histopathological, electron microscopy, cytogenetic and genetic studies [5–11].

Cytogenetic studies have shown that heterogeneity is related to karyotypic complexity. Common features are frequent occurrence of unbalanced rearrangements leading to genomic imbalances with losses and gains of certain chromosomes or chromosome regions. Moreover, alterations in the 9p21 locus and *TP53* gene are associated with CHS progression. The complete loss of *TP53* is accompanied by significant increase in the growth rate, karyotype instability and lack of genetic response in different tumors [12–14].

It is therefore important to find other parameters that can be of help in the stratification of the diagnosis and in the prognosis of these neoplasms. The aim of the present study is to describe the histopathological, immunohistochemical, ultrastructural, molecular biology and cytogenetic studies of a primary grade II chondrosarcoma; the new cell line established from the original tumor; and successive xenograft passages in nude mice.

Material & Methods

Case Report

A 25-year-old male was referred to our hospital complaining of pain in the left lumbar area. Computed axial tomography showed a 14×12×12 cm mass located in the left pelvis, affecting the iliac vein and causing a pulmonary thromboembolism (Fig. 1). There was no evidence of metastatic disease at the moment of diagnosis. Due to the location and the extension, a resection was not performed. A biopsy was made, establishing a WHO diagnosis of grade II chondrosarcoma. Tumor material was collected to perform the histopathologic characterization, and the ultrastructural and genetic studies. Moreover, the tumor was inoculated into nude mice. Neoadjuvant therapy (chemotherapy: ifosfamide-adriamicyn, temozolomide, gemcitabine-taxotere, celecoxib and dexamethasone; and radiotherapy) was administered, but the tumor progressed. Lung metastases were detected 2 months later and the patient died 1 year after the initial diagnosis. Approval for the study herein reported was provided by the institutional review board of our institution.

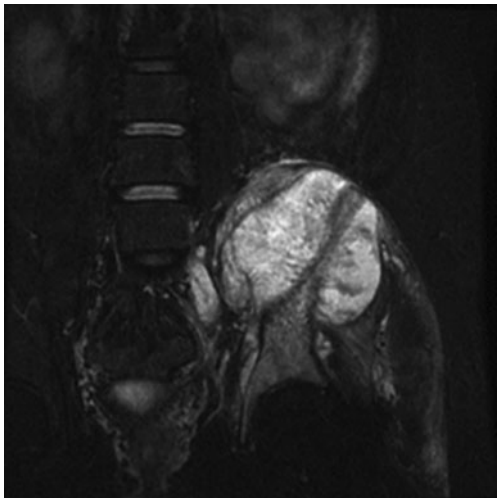

Fig. 1 Representative image of the tumor and the location (CT)

Xenotransplant

Male nude mice, were purchase from IFFA-CREDO (Lyon, France), kept under specific pathogen-free conditions throughout the experiment, and provided with vinyl isolates plus sterilized food, water, cage and bedding. The specimen for xenotransplant was obtained at biopsy; fragments of non-necrotic tumor, about 3 to 5 mm^3 in size, were transplanted into the subcutaneous tissue in the backs of two nude mice. The new tumor transfers were made following the same procedure as in the initial xenotransplant, and always under highly sterile conditions. Material from different passages was obtained in order to construct tissue microarrays (TMA). Additional material was obtained for electron microscopy, culture, and frozen sections. A total of 13 passages were made over a period of 26 months.

Cell Culture, Establishment of the CH-3573 Cell Line and Cytogenetic Studies

Tissue samples from the primary tumor were taken, dissected under aseptic conditions and immediately immersed in sterile RPMI 1640 medium (Gibco BRL, Grand Island, New York) supplemented with 2% antibiotics and 0.05 mg/ml of gentamicin sulfate. Samples of the tumors were rinsed gently twice in PBS (Gibco BRL) with 2% antibiotics and minced; the fragments were disaggregated using 0.2% collagenase type II for 30 min (Sigma-Aldrich, St. Louis, Missouri). The suspension obtained was diluted in RPMI 1640 medium supplemented with 20% fetal bovine serum, 1% L-glutamine (200 mM), 1% penicillin (50 U/ml) and streptomycin sulfate (50 μg/ml) (Gibco BRL). The cells were then seeded into 25 cm^2 tissue culture flasks (Nunc, Roskide, Denmark) containing 5 ml of complete medium, and maintained in a humidified atmosphere at 5% CO2 in

air at 37°C. The medium was replaced twice weekly. A confluent cell layer of the primary culture of the original tumor was obtained at day 7. Subcultures were then made with 0.25% trypsin-1 mM EDTA (Gibco BRL). Cells were stored under liquid N_2 in culture medium containing 5% dimethylsulfoxide (DMSO) (Sigma-Aldrich).

Normal growth kinetics were determined by trypsinizing the cultures in triplicate and resuspending the cells in medium. The viable cells were counted in a hemocytometer by dye exclusion with 0.1% trypan blue in PBS every 24 h for 4 days. Doubling time of the cell population was estimated in a logarithmic growth phase.

Cytogenetic analyses were made from a short-term culture of the primary tumor at 7 days of seeding, and at passages 4, 7, 14, 22, 33, 38, 46 and 60 of the cell line. Cells were prepared for karyotyping by incubating actively-growing cultures with 0.02 μg/ml of Colcemid (Gibco BRL) for 75 min before harvest. Cells were disaggregated with trypsin-EDTA (Gibco BRL), exposed to a hypotonic treatment of 0.075 M KCl at 37°C for 20 min, and then fixed three times with 3:1 methanol glacial acetic acid. Air-dried chromosome spreads were banded by the Giemsa-trypsin method. At least 25 metaphases were analyzed in each sample, and the karyotype was described according to guidelines of the International System of Human Cytogenetic Nomenclature (ISCN, 2005).

Tumorigenicity of the cell line was tested by heterotransplantation in 4- to 6-week-old nude mice with the1st, 40th and 60th cultured passages. An inoculum of 2×10^6 cells suspended in PBS was subcutaneously injected into their right flank.

To discard mycoplasma contamination, the CH-3573 cells were stained with Hoechst 33342 (5 μg/ml) (Sigma) for 10 min at 37°C and examined with a fluorescence microscope at x1000 under oil immersion.

Multicolor Fluorescence in situ Hybridization (COBRA-FISH)

Cells were isolated from the primary tumor and passages 14 and 20 from the cell line using mechanical and enzymatic dissociation procedures. The 43-color FISH staining of every chromosome arm in different color combinations with digital imaging and analysis were performed as previously described [15]. Hybridizations with individual whole chromosome painting probes labeled with single fluorochromes were used to confirm the detected re-arrangements. Chromosomal breakpoints were assigned by using inverted images counterstained with 4′,6-diamidino-2-phenylindole (DAPI) (Vysis, Downers Grove, Illinois) together with the information derived from the short- and long-arm-specific hybridization from the COBRA-FISH and FISH mapping data.

Histopathology and Immunohistochemistry

Three-μm thick sections of formalin-fixed paraffin-embedded tissue (FFPET) of the primary tumor and successive xenograft passages were used for conventional hematoxylin and eosin (H&E) and immunohistochemistry (IHC) stainings. A TMA was constructed including the original tumor and the successive tumor passages from xenografts. The TMA was assembled using a manual tissue arrayer (Beecher Instruments, Sun Prairie, WI), incorporating the two most representative areas of the primary tumor and of the thirteen xenografted nude mice passages (1 mm in diameter). A review and evaluation of whole sections as well as TMA sections was performed on hematoxylin and eosin (H/E) stained slides to study the histological variables. The IHC analysis was performed in primary tumor, culcured cells and xenografts using the Streptavidin-Biotin-Complex (sABC) method. The antibodies used are shown in Table 1. Antigen retrieval was performed by pressure cooker boiling for 3 min in 10 mmol/L of citrate buffer (pH 6.0). The LSAB method (DakoCytomation) was used, followed by revelation with 3,3′-diaminobenzidine. Moreover, Alcian blue, toluidine blue and PAS stainings were made on TMAs. Sections were examined and the immunoreactivity was defined as follows: negative, fewer than 5% of tumor cells stained; poorly positive (+), 5% to 10% of tumor cells stained; moderately positive (++), 10% to 50% of tumor cells stained and strongly positive (+++), more than 50% of the tumor cells stained.

Electron Microscopy

For transmission electron microscopy, tissue was fixed in glutaraldehyde, postfixed in 1% osmium tetroxide, dehydrated in graded alcohols, and embedded in Epon (Polysciences Europe GmbH, Eppelheim, Germany).The samples were cut into 1 μm-thick sections and stained with toluidine blue in order to select the most representative areas from the primary tumor, cultured cells and xenografts by optical microscopy. Ultrathin sections were examined using a Jeol 100B microscope (Tokyo).

Molecular Biology

Expression studies (RNA-based tests):

We decided to study the cell cycle genes because mutations in these genes were found to correlate with incorrect cell division and it is well established that they constitute a frequent event in these neoplasms [14, 16]. Total RNA was extracted from frozen tissues and cultured cells using TRIzol reagent (Gibco-BRL) and the Pure Link RNA Mini kit (Invitrogen, San Diego, CA, USA) according to the manufacturer's instructions and dissolved in 60 μl of RNAsa-free

Table 1 Principal characteristics of the antigens used in our study

Ag	Monoclonal/ Polyclonal	Clone	Dilution	Location	Ag. retroviral	Source
CD99	monoclonal	clone 12E7	1:50	cytoplasmic	Yes	Dako Cytomation
S-100	polyclonal		1:1000	nuclear	No	Dako Cytomation
SOX-9	polyclonal		1:100	nuclear	No	Santa Cruz Biotechnology
COX-2	polyclonal		1:50	nuclear	No	Santa Cruz Biotechnology
P16	monoclonal	clone F12	1:100	nuclear	No	Santa Cruz Biotechnology
P21	polyclonal		1:50	nuclear	Yes	Santa Cruz Biotechnology
P27	monoclonal	clone SX53G8	1:50	nuclear	No	Dako Cytomation
P53	monoclonal	clone DO7	1:50	nuclear	Yes	Novocastra
Ki-67	monoclonal	1:50	1:50	nuclear	Yes	Dako Cytomation
MDM2	monoclonal	IB10	1:50	nuclear	Yes	Novocastra
Ezrin	monoclonal	clone 3 C12	1:250	cytoplasmic	No	Santa Cruz Biotechnology
Caveolin	polyclonal		1:200	cytoplasmic	Yes	Santa Cruz Biotechnology
Estrogen	monoclonal	clone 6 F11	1:40	nuclear	No	Novocastra
CAM 5.2	monoclonal	clone 5D3	1:50	cytoplasmic	Yes	Novocastra
EMA	monoclonal	clone 29	1:200	cytoplasmic	Yes	

water. DNA was extracted from 0.10–0.15 g of fresh frozen tissue and cultured cells using the QIAmp DNA Mini Kit (Qiagen, Inc., Valencia, CA) following the manufacturer's instructions. Once RNA and DNA were obtained these were quantified by NanoDrop® 1000 spectrophotometer. The primers for all studies have been described previously [17]. For the RNA studies, reverse transcription was performed on 200 ng total RNA using the Qiagen OneStep RT-PCR Kit (Qiagen) using primers described for the *EWS-CHN* and *TAF2-CHN* fusions [18]. The integrity of the RNA for the RT-PCR was confirmed by amplification of the *β-globin*. Moreover, we analyzed the retinoblastoma alterations [16] and expression of *p21*, *p27* and *D-type cyclins* (D1, D2 and D3) [16] by reverse transcription, performed on 200 ng total RNA using the High Capacity cDNA Reverse Transcription Kit (Applied Biosystems, Inc, Foster City, CA).

Genome tests (DNA-based studies):

Sequencing Analysis, version 5.2 software (Applied Biosystems) and the National Center for Bioinformatics Information blast tool (http://www.ncbi.nlm.nih.gov/BLAST/) were used to confirm the mutation sequences using the following Ensembl (http://www.ensembl.org/Homo_sapiens/index.html) reference sequences for Rb (GenBank accession number: NM_000321).

DNA was used to analyze molecular alterations of the G1 to S phase cell cycle transition as previously described [17]. dPCR was used to detect homozygous deletion of the 9p21 locus genes: the presence of homozygous deletion was confirmed by the loss of the PCR product corresponding to $p15^{INK4B}$, $p16^{INK4A}$, and $p14^{ARF}$ genes with the presence of microglobulin amplification. The methylation status of the 5'CpG island in the promoter region of the $p15^{INK4B}$, $p16^{INK4A}$, and $p14^{ARF}$ genes was determined using the Methylamp One-Step DNA Modification Kit (Epigentek, Bio Nova, Spain) and following the manufacturer's instructions. Gene amplification of the MDM2, CDK4, NMYC and Cyclin D1 genes was determined by dPCR using two sets of primers, one corresponding to the target gene and the other to an internal control gene (*β-globin*).

Identification of *TP53* mutations was performed by direct sequencing of exons 5 to 8 of the gene on an ABI310 sequencer using the Big Dye Terminator v1.1 kit (Applied Biosystems, Inc, Foster City, CA). Sequencing Analysis, version 5.2 software (Applied Biosystems) and the National Center for Bioinformatics Information blast tool (http://www.ncbi.nlm.nih.gov/BLAST/) were used to confirm the mutation sequences using the following Ensembl (http://www.ensembl.org/Homo_sapiens/index.html) reference sequences for *TP53* (GenBank accession number: AF307851).

Fluorescence in situ Hybridization (FISH)

The *TP53* FISH study was performed to clarify the molecular and IHC results. The samples for *TP53* FISH analysis

(P53 (17P13)/SE 17 Kreatech, Amsterdam, the Netherlands) were studied by TMA and metaphases of the passage 14 in the cell line. The slides for FISH were prepared 1 day before performing the assay. Hybridization and detection of the hybridization signals were performed according to the manufacturer's instructions. Counterstaining of metaphases was done with DAPI. The green and red hybridization signals were counted in all TMA regions, counting a minimum of 100-200 non-overlapping nuclei. The fluorescent signals were detected using a Zeiss Axioplan 2 fluorescence microscope and an in situ imaging system Isis (Carl Zeiss Vision, Oberkochen, Germany).

Results

Morphologic Studies in the Primary Tumor

The histopathology revealed an intermediate grade tumor with high cellularity, presence of plump cells with double nuclei, areas with atypical chondroblast and spindle cells. Tumor cells were suspended in a myxoid/chondroid matrix. The cells were vaguely arranged in cords and nests, with a pale, eosinophilic cytoplasm and a round, hyperchromatic nucleus. Focally, especially in the areas permeating the trabeculae of the bone, the tumor disclosed a more chondroid appearance with a dense, eosinophilic matrix and large atypical chondrocytes.

The mitotic rate was low, and no necrosis was observed in the original tumor. Soft tissue infiltrations of chondroid nests with atypia were detected. The tumor was diagnosed as central chondrosarcoma Grade II.

Ultrastructurally, the primary tumor showed an abundant intra and intercellular matrix. A pseudobasal lamina was found focally, partially surrounding some cells. The tumor cells had round or slightly irregular-shaped nucleus with peripheral dense chromatin and large nucleoli. The cytoplasm contained abundant rough endoplasmic reticulum, arrays of parallel microtubules, and occasional bundles of filaments. The cultured cells showed a smooth surface and polygonal or spindle contour (Fig. 2j). They appeared closely packed to one another, forming clusters without specific cell-to-cell attachments or rudimentary tight junctions. The cells had round or oval nuclei with fine, dispersed chromatin and one or two prominent nucleoli and a scarce cytoplasm poor in organelles. Glycogen and intermediate filaments were seen, as well as numerous small lipid droplets. Matrix production was observed in all the passages of the CH-3573 cultured cells.

Morphologic Studies in Xenograft Nude Mice

In nude mice inoculated with fragments of primary tumor, solid tumor masses were observed at 124 days. Thirteen passages were made over a period of 32 months. Morphologically, the xenografted tumors did not show any significant variation compared with the original tumor. In the initial and middle passages of xenografts the tumor morphology did not change, and an evident chondroid matrix formation was detected. The matrix formation was retained, even though the tumor became more undifferentiated in the later passages, with an increase in the number of atypical chondrocytes and higher mitotic rate. Ultrastructurally, immature mesenchymal-chondroid cells were seen vaguely packed in a stroma with flocculent material. The cells had cytoplasm with isolated vacuoles, lipid droplets, glycogen, and intermediate filaments. The nucleus was large, with a round or invaginated contour and fine chromatin. Occasionally, membrane attachments with poorly differentiated desmosomes and deposits of amorphous dense material associated with collagen bands were observed.

The injection of CH-3573 cells into nude mice induced a visible solid tumor at the site of inoculation after 30 days, which gradually enlarged. Microscopically and ultrastructurally the tumor presented as conventional CHS, although it was more dedifferentiated. The cells retained their proliferative activity. Intratumoral blood vessels and some necrotic areas were present (Figs. 3 and 4).

Cytogenetic Studies

In the original tumor 25 metaphases were counted: 11 metaphases were in the hypodiploid range with a modal chromosome number of 37 and displayed several chromosomal anomalies and 14 metaphases revealed a normal male karyotype. In the first xenografted passage, 12 metaphases were counted with similar anomalies of the original tumor and polyploidization (~20%). The karyotype of the different passages was analyzed, observing a polyploidization in the majority of metaphases showing a modal chromosome number of 74 (~90%). We observed loss of chromosomes 2, 4, 5, 10, 12, 13, 15, 17, 19 and 22; and complex structural rearrangements affecting chromosomes 1, 5, 6, 8, 11, 13, 14, 17, 18, 19 and 20. High chromosomal instability was observed with chromosomal loss and numerous structural rearrangements.

COBRA-FISH Studies

Based on G-banding and the COBRA-FISH studies the karyotype of the cells could be formuled as follows: 32-38,X,der(Y)t(Y;19)(p11;p11),der(1)t(1;16)(p12;p11),der(1;22) (q10;q10)t(3;22)(q;q)t(3;15)(q?;q?),der(2)t(2;?:8)(p13;?;q23),der(3;6)(q10;q10)t(6;12) (q27;q24.3),-4,der(5)t(5;13)(p10;p10),-6,i(8)(q10),der(8)t(8;19)(p23;p13),der(10;17) (p10;p10),-11,der(12)t(11;12)(p13;q13),-13,ider(13)(13q31::2p::17?::13q10::13q10 ::13q?::2p?::17?::13q??::

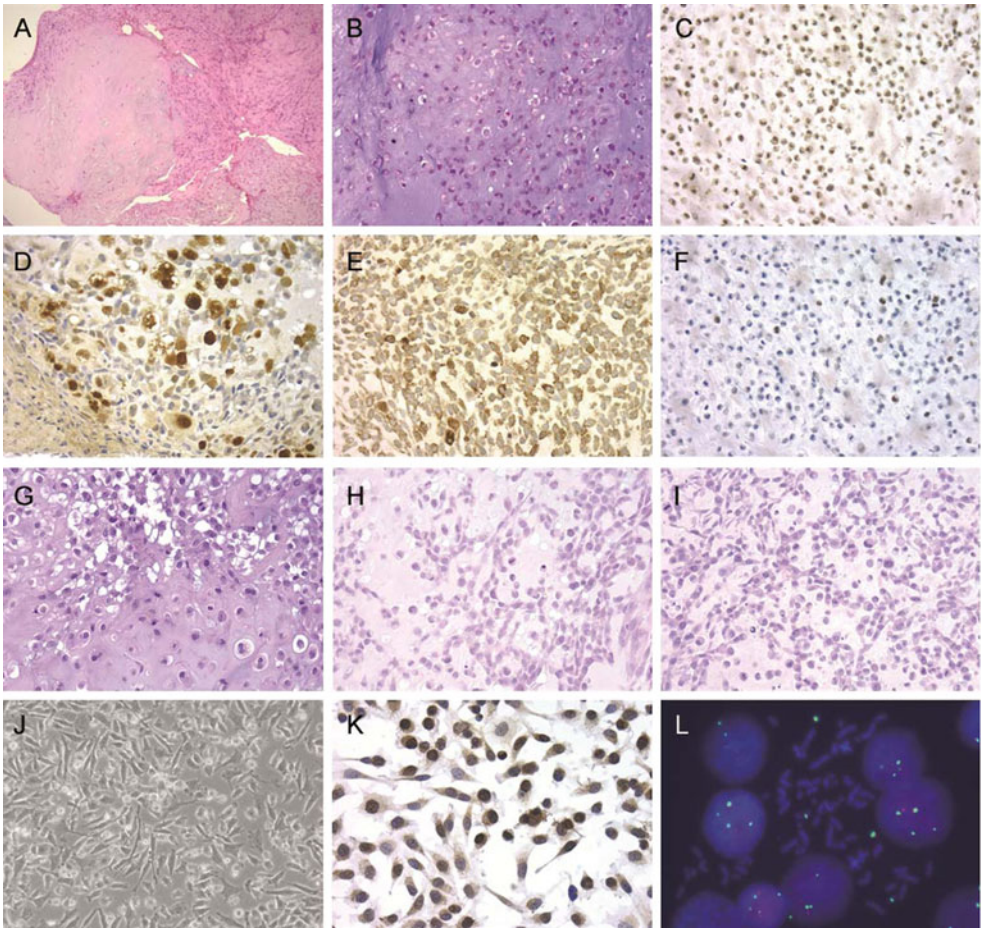

Fig. 2 Principal characteristics of our Chs. First and second rows: primary tumor, **a** H&E10X, **b** H&E 40X, (**c**) SOX-9 moderate positivity 40X, **d** S-100 moderate positivity 40X, **e** ezrin intense positivity 40X, **f** Ki-67 expression <10%. Third row: initial **g**, intermediate **h** and final **i** nude mice passages at 40X. Bottom row: cell line in culture at passage 8 at 10X **j**, SOX-9 intense positive **k** and p53 FISH in metaphase **l**

1q23-qter),der(14)t(14;15)(q32;q11),-15,-15,-16,-17,der(17;17) (q10;q10)t(16;17)(q21;q12),-18,-19,der(20)t(10;17)(p;p11)t(10;20)(?;p11),der(21)(7;21) (q31.2;q22.3),-22/idemx2 (Fig. 3).

Immunohistochemical Characterization

The primary tumor, the xenografts and the cell line all expressed SOX-9, CD99, ezrin, MDM2, COX2 and Ki-67.

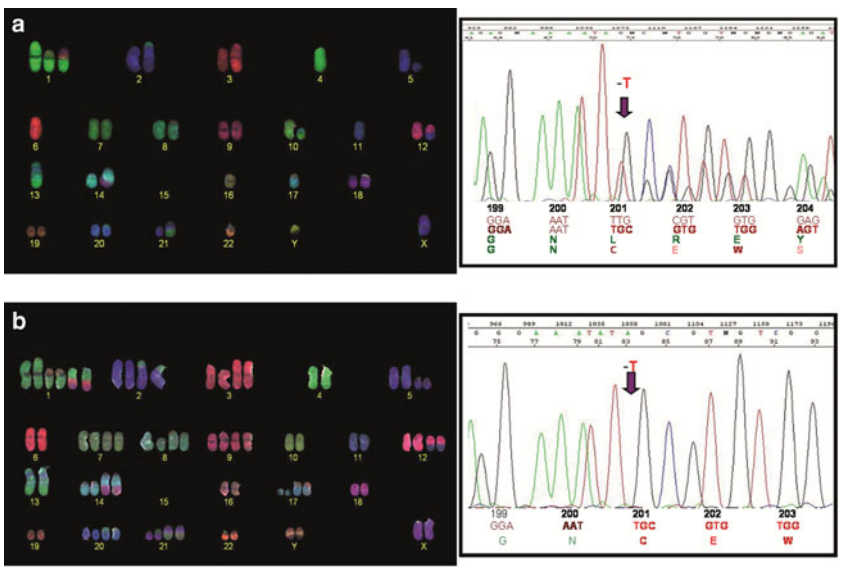

Fig. 3 COBRA-FISH of the primary tumor and heterozygous mutation in p53 **a**. Homozygous mutation in p53 and COBRA-FISH in the passages **b**

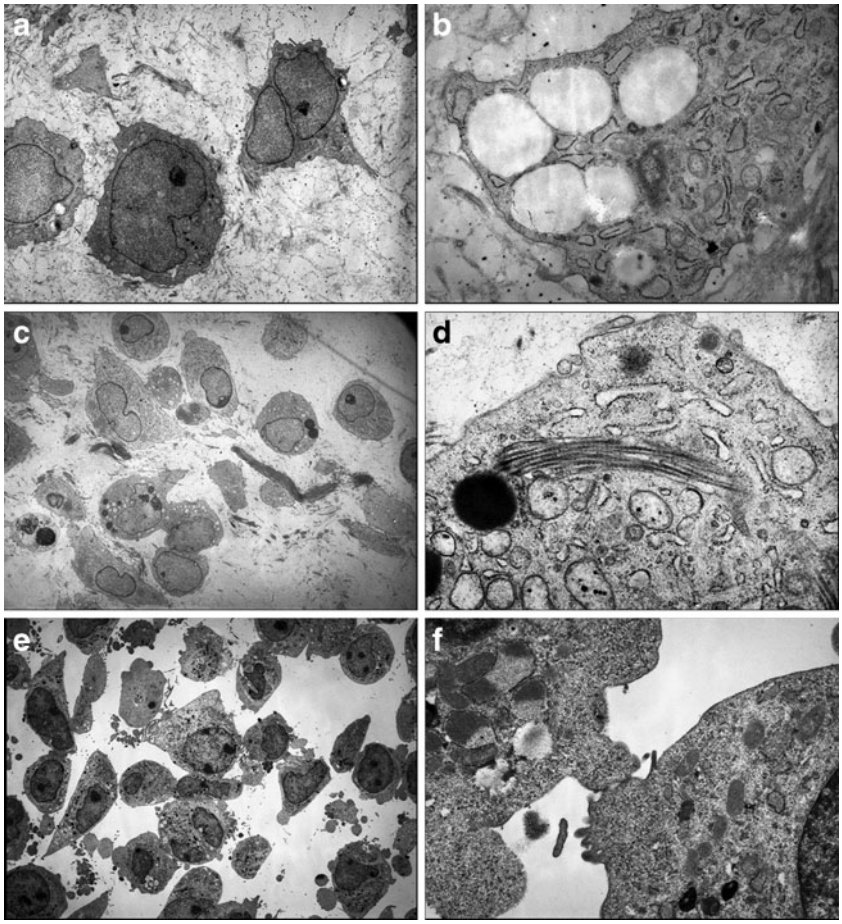

Fig. 4 Electron microscopy, primary tumor **a**-**b** showing the ground substance, residual bodies, lipid droplets and endoplasmic reticulum. Xenograft passages **c**-**d** showing collagen synthesis and cytoplasmic inclusions. Culture cells **e**-**f** with inclusion bodies, secretory activity and lipid production

However, p53, S-100, EMA, CAM 5.2, estrogen, caveolin-1, P27 and P21 were not expressed (Fig. 2) (Table 2). Toluidine blue and Alcian blue staining confirmed the presence of matrix production in the original tumor and successive xenograft passages.

Molecular Biology Studies

Analysis of RNA by RT-PCR did not reveal an *EWS-CHN* product in any of the samples analyzed. No homozygous deletion of the 9p21 locus genes ($p16^{INK4A}$, $P14^{ARF}$ and $P15^{INK4B}$) was found in any of the samples. No hypermethylated status in the 5'CpG island of the $p16^{INK4A}$, $P14^{ARF}$ and $P15^{INK4B}$ genes was detected. No genetic amplifications of *NMYC*, *MDM2*, *CCND1* or *CDK4* and *RB1* mutation genes were observed in any of the analyzed samples. Mutational status of *TP53* showed a deletion of the second T in codon 201 in exon 6 which produced a STOP codon at 246 and correlated with the loss of *p21WAF1/Cip1* gene expression. This mutation was heterozygous in primary tumor and first passage of xenografts and cell line, and homozygous in other passages, both in xenografts and the cell line (Fig. 3).

Fluorescence in situ Hybridization

TP53 was studied by FISH because chromosome 17 presented multiple anomalies in the karyotype as well as a mutation in exon 6. This analysis demonstrated one red signal that corresponded to the *TP53* gene, and two green signals corresponding to the centromeric chromosome 17 in the primary tumor and first passages; as well as double red signals corresponding to gene *TP53* and four green signals corresponding to the centromeric chromosome 17 in the remaining passages, all of which had a duplicate karyotype (Fig. 2l).

Discussion

We describe the establishment and detailed characterization of a grade II CHS cell line (CH-3573) with abundant matrix production which was maintained in the xenografts after several passages in vivo and in vitro. The histopathology, immunohistochemistry and electron microscopy results did not reveal any significant variation between the original tumor, subsequent xenografted passages, cell line passages

Table 2 Immunohistochemical results in the primary tumor; initial, middle and last passages of the nude mice; cell line (CH-3573) and inoculated cell lines in nude mice (465 cell line)

IHC	Primary tumor	465-1 Initial nude	465-6 middle nude	465-13 final nude	CH-3573	465-cell line
SOX-9	+++	–	–	+++	+++	+++
KI-67	+	+	+	+++	+++	+++
P53	–	–	–		–	–
CD 99	++	++	–	++	+++	+++
EZRIN	+++	–	–	+++	+++	+++
S-100	+	+	–	+	+	+
MDM-2	–	–	+	+	–	+
CAM 5.2	–	–	–	–	–	–
EMA	–	–	–	–	–	–
ESTROGEN	–	–	–	–	–	–
CAVEOLIN	–	–	–	–	–	–
P21	–	–	–	–	–	–
P27	++	++	–	–	–	–

and inoculation cell line in nude mice. Although cell lines are described from high-grade or undifferentiated CHS [8–11], to our knowledge, no report has so far described the establishment of a cell line from a grade II CHS with preserved matrix production. A cell line with these characteristics represents an excellent model for gaining knowledge in the pathogenesis and biology of this neoplasm and could constitute a useful method for identifying potential targets for directed therapies which could improve the outcome of CHS patients.

Cytogenetic studies have revealed considerable heterogeneity with respect to karyotypic complexity. CHS karyotypes may range from simple numerical changes to abundant, complex numerical and structural abnormalities [19, 20]. Despite this heterogeneity, however, involvement of certain chromosomal bands or regions seems to be recurrent. The following imbalances were detected in aberrant CHS: loss of chromosomes or chromosomal regions 1p36, 1p13~p22, 4, 5q13~q31, 6q22~qter, 9p22~pter, 10p, 10q24~qter, 11p13~pter, 11q25, 13q21~qter, 14q24~qter, 18p, 18q22~qter, and 22q13 and gain of 7p13~pter, 12q15~qter, 19, 20pter~q11, and 21q [10, 20]. Abnormalities of 9p and extra copies of chromosome 22 are prominent in central CHS versus peripheral CHS [21]. Previously, chromosomal aberrations of 6q13~q21 have been proposed to correlate with locally aggressive behaviour in both benign and malignant cartilaginous neoplasms [4]. Mandahl et al. have reported loss of material from 13q as a predictor of metastasis, regardless of tumor size or grade [20]. Due to the heterogeneity and complexity of the CHS karyotype, there are no single characteristic numerical or structural rearrangements, alterations or anomalies in grade II CHS, with the exception of extraskeletal myxoid CHS. However, the copy number imbalance does not affect metastasis or tumor-associated death [22]. Malignant transformation and progression of cartilage tumors seems to be associated with an increasing incidence of clonal chromosome aberrations, reflecting the multistep process of tumor development, involving activation of oncogenes, loss of tumor suppressor genes, and secondary or tertiary genetic alterations. In the present case, the cytogenetic studies showed that the primary tumor had a hypodiploid karyotype and consecutive polyploidization in the primary passages of the cell line as well as the xenografts. CH-3573 presented losses of chromosomes, complex structural rearrangements and clonal numerical abnormalities. For the identification of these complex structural rearrangements we used a multicolour-FISH-based karyotyping tool (COBRA-FISH). It is very important to use complementary techniques to explain tumor progression in the different types of neoplasms and patients. Only chromosomes 1q, 7, 9 and 18 were disomic in our case. In more than one-fourth of the investigated cases of CHS, the regions affected by chromosomal imbalances included gain of parts of chromosomes 5, 12 and 19 to 22 and loss of parts of chromosomes 1, 4, 6, 9 to 11, 14, and 17 and the whole chromosome arm 13q; although these regions most probably harbour genes of importance for chondrosarcoma development [19, 20].

In CHS, abnormalities of chromosome 1 have been reported as being the most common secondary alteration. However, it is important to note that rearrangements involving chromosome 1 have been frequently observed in several other tumor types such as leiomyosarcomas, colorectal adenocarcinomas, and breast carcinomas, most frequently resulting in the loss of terminal 1p segments [19]. Other reported alterations in order of frequency would be chromosome 16, 22, 3 15 and 21.

A recurrent amplicon was also identified in 11q22.1-q22.3, affecting a region harboring a cluster of MMP genes,

which encode matrix metalloproteinases. We observed matrix production in the primary tumor, xenografts and cell line, however, karyotyping showed loss of one chromosome 11 and a derivative chromosome 11 of translocation between chromosome 11 and 12, der(12)t(11;12). We confirmed with karyotyping and molecular biology that no amplification of 12q13 region was present. This region has several genes important in cell cycle control including *CDK4* and *MDM2*, although this region correlates with high histological grade [23, 24].

Genetic mutations in the regulatory genes implicated in cell cycle control can be considered to target one of two critical pathways: the Rb pathway that regulates G1/S-phase transition and p53 pathway that induces growth arrest or apoptosis in response to either DNA damage or inappropriate mitogenic stimuli. Molecular alterations of the integrating elements of either pRb, p53, or both pathways suppress their normal function, abrogating regulation of cell cycle transition from G1 to S-phase and driving cells to proliferation.

A key regulatory function of the *TP53* gene, the ability to arrest the cell cycle, occurs with proper activation of the retinoblastoma (*RB1*) pathway. Studies for LOH on 13q and/or *RB1* gene mutations in CHS are scarce [25–27]. In one study, a significant association between local recurrence and LOH on 13q was seen in grades I–II CHS. (25] Our case had a loss of chromosome 13 and at 2 months metastasised to the lung. It has also been suggested that loss of 13q is a factor of worse prognosis [20], and exerts an influence regardless of tumor size or histopathologic grade. This parameter could be important in identifying patients who require intensified treatment. However, in this case, the *pRb* (13q14.2) level was normal, without mutations; possibly because the unidentified marker in the karyotype consisted in part of the chromosome 13q14.

Cyclin-dependent kinase (Cdk) inhibitory molecules are capable of blocking *pRb* phosphorylation; in our case no alteration was observed in *CDK4* or *Cyclin D1*. Deletions of the p16 (*CDKN2A*) gene and/or the p15 (*CDKN2B*; alias *MTS2*) gene, members of the Cdk inhibitory molecule family, have been observed in a small subset of primary CHS and CHS cell lines.[28–30] Moreover, genomic loss of the chromosomal locus for the p16 and p15 genes, located at 9p21, has been detected by CGH analysis, though in a small number of cases (10%) [22, 24], and is frequently rearranged cytogenetically, particularly in central CHS [21]. Changes in *p14ARF* do not play a primary role in CHS [31]. Although amplifications and homozygous deletions were relatively infrequent findings, these mechanisms seem to be important in a subset of grade III CHS. In our cases, the deletions and methylation of the 9p21 ($p16^{INK4A}$, $P14^{ARF}$ and $P15^{INK4B}$) were exhaustively analysed. The loss of function in the encoded protein is an infrequent finding in CHS, in line with this fact, no alteration was detected in our cases, indicating that in many aspects this cell line represents CHS with more frequently-occurring genetic profiles [32]. Furthermore, it is noteworthy that the intrinsic resistance of chondrosarcoma cells to radiation therapy has been suggested to be in part due to loss of this region [33].

Mutation screening of the TP53 gene revealed a deletion of the second T in codon 201 in exon 6 resulting in a STOP codon at 246. From all tested tumor suppressor gene and oncogene alteration (mutation/deletion, gains) alterations of *TP53* were the only positive finding in our cell line. Mutation of this gene has been found in a subset of CHS and is mostly associated with aggressive behaviour [34]. In the karyotype study of primary tumor two copies of rearranged chromosome 17 were present; furthermore a hemizygous deletion of the *TP53* allele was detected by locus specific FISH. In the primary tumor a low percentage of normal signals (*TP53* and centromere of chromosome 17, 2:2) was observed; indicating that the *TP53* status was already biclonal of the primary tumor sample. In the xenograft cell line tumor cells carrying a hemizygous loss of one allele and mutation of the other allele resulting in complete inactivation of the p53 occurred. This clonal evolution of the more aggressive clone which carries a homozygous inactivation of the *TP53* gene was accompanied by a significant increase in the growth rate and gain of karyotypic instability. In our case, the *TP53* mutation produced a mitogenic signalling and consequently a hyperdiploid population was established in culture, originating from the hyperdiploid clone through endomitosis or endoreduplication. This fact suggests that polyploidization, common in CHS, is an evolutionary pathway and has been associated with further progression toward high-grade CHS [35]. As with our other cell line, CH2879, polyploidization, occurring in the first passage of the xenotransplanted tumor and early in the cell line, would represent, by the acquisition of two copies of the monosomic chromosomes, a selective advantage for those cells that have undergone extensive loss of heterozygosity [10].

In conclusion, we report the establishment and detailed molecular, genetic and functional characterisation of a new grade II CHS cell line (CH-3573) with retained matrix production capability. This sample may serve as an important tool for additional studies related to tumorigenesis, drug response, immune response, angiogenesis and in vivo/in vitro differentiation studies.

Acknowledgements We would like to thank Ms. Elisa Alonso, Ms. Ana Clari and Ms. Laura Martínez for their technical assistance.

Grant numbers and sources of support This study was supported by and performed within the project EuroBoNeT Network (Contract nº 018814) from 6th FP of the European Community.q+

References

1. Evans HL, Ayala AG, Romsdahl MM (1977) Prognostic factors in chondrosarcoma of bone: a clinicopathologic analysis with emphasis on histologic grading. Cancer 40(2):818–31
2. Rozeman LB, Cleton-Jansen AM, Hogendoorn PC (2006) Pathology of primary malignant bone and cartilage tumour. Int Orthop 30 (6):437–44
3. Puri A, Shah M, Agarwal MG, Jambhekar NA, Basappa P (2009) Chondrosarcoma of bone: does the size of the tumor, the presence of a pathologic fracture, or prior intervention have an impact on local control and survival? J Cancer Res Ther 5(1):14–9
4. Riedel RF, Larrier N, Dodd L, Kirsch D, Martinez S, Brigman BE (2009) The clinical management of chondrosarcoma. Curr Treat Options Oncol 10(1–2):94–106
5. Takigawa M, Tajima K, Pan HO et al (1989) Establishment of a clonal human chondrosarcoma cell line with cartilage phenotypes. Cancer Res 49(14):3996–4002
6. Takigawa M, Pan HO, Kinoshita A, Tajima K, Takano Y (1991) Establishment from a human chondrosarcoma of a new immortal cell line with high tumorigenicity in vivo, which is able to form proteoglycan-rich cartilage-like nodules and to respond to insulin in vitro. Int J Cancer 48(5):717–25
7. Ikemoto S, Sugimura K, Yoshida N, Nakatani T (2004) Chondrosarcoma of the urinary bladder and establishment of a human chondrosarcoma cell line (OCUU-6). Hum Cell 17(3):93–6
8. Kudo N, Ogose A, Hotta T et al (2007) Establishment of novel human dedifferentiated chondrosarcoma cell line with osteoblastic differentiation. Virchows Arch 451(3):691–9
9. Yang L, Chen Q, Zhang S, Wang X, Li W, Wen J et al (2009) A novel mutated cell line with characteristics of dedifferentiated chondrosarcoma. Int J Mol Med 24(4):427–35
10. Gil-Benso R, Lopez-Gines C, Lopez-Guerrero JA et al (2003) Establishment and characterization of a continuous human chondrosarcoma cell line, ch-2879: comparative histologic and genetic studies with its tumor of origin. Lab Invest 83(6):877–87
11. Kalinski T, Krueger S, Pelz AF et al (2005) Establishment and characterization of the permanent human cell line C3842 derived from a secondary chondrosarcoma in Ollier's disease. Virchows Arch 446(3):287–99
12. Oshiro Y, Chaturvedi V, Hayden D et al (1998) Altered p53 is associated with aggressive behavior of chondrosarcoma: a long term follow-up study. Cancer 83(11):2324–34
13. Terek RM, Healey JH, Garin-Chesa P, Mak S, Huvos A, Albino AP (1998) p53 mutations in chondrosarcoma. Diagn Mol Pathol 7 (1):51–6
14. Scully SP, Layfield LJ, Harrelson JM (1997) Prognostic markers in chondrosarcoma: evaluation of cell proliferation and of regulators of the cell cycle. Sarcoma; 1(2):79–87
15. Szuhai K, Tanke HJ (2006) COBRA: combined binary ratio labeling of nucleic-acid probes for multi-color fluorescence in situ hybridization karyotyping. Nat Protoc 1(1):264–75
16. Lopez-Guerrero JA, Lopez-Gines C, Pellin A, Carda C, Llombart-Bosch A (2004) Deregulation of the G1 to S-phase cell cycle checkpoint is involved in the pathogenesis of human osteosarcoma. Diagn Mol Pathol 13(2):81–91
17. Lopez-Guerrero JA, Pellin A, Noguera R, Carda C, Llombart-Bosch A (2001) Molecular analysis of the 9p21 locus and p53 genes in Ewing family tumors. Lab Invest 81(6):803–14
18. Okamoto S, Hisaoka M, Ishida T et al (2001) Extraskeletal myxoid chondrosarcoma: a clinicopathologic, immunohistochemical, and molecular analysis of 18 cases. Hum Pathol 32(10):1116–24
19. Tallini G, Dorfman H, Brys P et al (2002) Correlation between clinicopathological features and karyotype in 100 cartilaginous and chordoid tumours A report from the Chromosomes and Morphology (CHAMP) Collaborative Study Group. J Pathol 196(2):194–203
20. Mandahl N, Gustafson P, Mertens F et al (2002) Cytogenetic aberrations and their prognostic impact in chondrosarcoma Genes Chromosomes. Cancer 33(2):188–200
21. Bovee JV, Sciot R, Dal Cin P et al (2001) Chromosome 9 alterations and trisomy 22 in central chondrosarcoma: a cytogenetic and DNA flow cytometric analysis of chondrosarcoma subtypes. Diagn Mol Pathol 10(4):228–35
22. Hallor KH, Staaf J, Bovee JV et al (2009) Genomic profiling of chondrosarcoma: chromosomal patterns in central and peripheral tumors. Clin Cancer Res 15(8):2685–94
23. Rozeman LB, Szuhai K, Schrage YM et al (2006) Array-comparative genomic hybridization of central chondrosarcoma: identification of ribosomal protein S6 and cyclin-dependent kinase 4 as candidate target genes for genomic aberrations. Cancer 107 (2):380–8
24. Larramendy ML, Tarkkanen M, Valle J et al (1997) Gains, losses, and amplifications of DNA sequences evaluated by comparative genomic hybridization in chondrosarcomas. Am J Pathol 150 (2):685–91
25. Yamaguchi T, Toguchida J, Wadayama B et al (1996) Loss of heterozygosity and tumor suppressor gene mutations in chondrosarcomas. Anticancer Res 16(4A):2009–15
26. Eisenberg MB, Woloschak M, Sen C, Wolfe D (1997) Loss of heterozygosity in the retinoblastoma tumor suppressor gene in skull base chordomas and chondrosarcomas. Surg Neurol 47 (2):156–60, discussion 60-1
27. Gunawan B, Weber M, Bergmann F, Wildberger J, Niethard FU, Fuzesi L (2000) Clonal chromosome abnormalities in enchondromas and chondrosarcomas. Cancer Genet Cytogenet 120(2):127–30
28. Asp J, Inerot S, Block JA, Lindahl A (2001) Alterations in the regulatory pathway involving p16, pRb and cdk4 in human chondrosarcoma. J Orthop Res 19(1):149–54
29. Jagasia AA, Block JA, Qureshi A et al (1996) Chromosome 9 related aberrations and deletions of the CDKN2 and MTS2 putative tumor suppressor genes in human chondrosarcomas. Cancer Lett 105(1):91–103
30. Jagasia AA, Block JA, Diaz MO et al (1996) Partial deletions of the CDKN2 and MTS2 putative tumor suppressor genes in a myxoid chondrosarcoma. Cancer Lett 105(1):77–90
31. Asp J, Brantsing C, Benassi MS et al (2001) Changes in p14(ARF) do not play a primary role in human chondrosarcoma tissues. Int J Cancer 93(5):703–5
32. Schrage YM, Lam S, Jochemsen AG et al (2009) Central chondrosarcoma progression is associated with pRb pathway alterations: CDK4 down-regulation and p16 overexpression inhibit cell growth in vitro. J Cell Mol Med 13(9A):2843–52
33. Moussavi-Harami F, Mollano A, Martin JA et al (2006) Intrinsic radiation resistance in human chondrosarcoma cells. Biochem Biophys Res Commun 346(2):379–85
34. Rozeman LB, Hogendoorn PC, Bovee JV (2002) Diagnosis and prognosis of chondrosarcoma of bone. Expert Rev Mol Diagn 2 (5):461–72
35. Bovee JV, van Royen M, Bardoel AF et al (2000) Near-haploidy and subsequent polyploidization characterize the progression of peripheral chondrosarcoma. Am J Pathol 157(5):1587–95